3D printed clamps for fixation of spinal segments in biomechanical testing

Originally published in:
Journal of Biomechanics 125, https://doi.org/10.1016/j.jbiomech.2021.110577

Journal of Biomechanics 125 (2021) 110577

Contents lists available at ScienceDirect

Journal of Biomechanics

journal homepage: www.elsevier.com/locate/jbiomech

3D printed clamps for fixation of spinal segments in biomechanical testing

Frédéric Cornaz [a,b], Marco Burkhard [a], Marie-Rosa Fasser [a,b], José Miguel Spirig [a], Jess Gerrit Snedeker [a,b], Mazda Farshad [a], Jonas Widmer [a,b,*]

[a] Department of Orthopaedics, Balgrist University Hospital, 8008 Zurich, Switzerland
[b] Institute for Biomechanics, ETH Zurich, 8093 Zurich, Switzerland

ARTICLE INFO

Keywords:
Biomechanical
Spine
Testing
Fixture
Anchoring
Sacrum
Lumbar
3D printed clamp

ABSTRACT

3D printed clamps provide multiple advantages compared to potting for the fixation of spinal specimens and in a recent study, superior fixation stability was reported. The aim of this study was to evaluate the fixation efficacy of 3D printed vertebra clamps during routine application and to present and evaluate a novel clamp for sacrum fixation. Further, public access to the template files is provided. 98 human single-level cadaveric specimens were biomechanically tested in flexion–extension (FE), lateral bending (LB), axial rotation (AR), anteroposterior shear (AS), lateral shear (LS) and axial compression-decompression (AC). Loading amplitudes were +/-7.5 Nm for FE, LB and AR, +/- 150 N for AS and LS and + 400/-100 N for AC. The novel sacrum clamp was used in 8 specimens. The median relative motion between clamps and specimens was 0.6° in FE, 0.7° in LB, 0.3° in AR, 0.5 mm in AS, 0.5 mm in LS and 0.1 mm in AC. With sacrum clamps, the median relative motion was 0.3° in FE, 0.1° in LB, 0.08° in AR, 0.8 mm in AS, 0.7 mm in LS and 0.2 mm in AC. The vertebra clamps used during routine testing provided better stability compared to the values in the literature in all six loading directions ($p < 0.05$). The sacrum clamp showed superior anchoring stability in three loading directions compared to the caudal vertebra clamps ($p < 0.05$), while inferior stability was measured in AS ($p < 0.001$). We conclude that 3D printed vertebra clamps and 3D printed sacrum clamps represent reliable methods for specimen fixation during routine biomechanical testing.

1. Introduction

Biomechanical experiments on spinal segments are an indispensable method to analyze the mechanical characteristics of the spine, to evaluate spinal implants and to validate numerical models. To record accurate data, a rigid and reproducible specimen fixation method is mandatory. Recently, 3D-printed clamps have been proposed as an alternative to traditional potting techniques for the fixation of thoracic and lumbar spinal segments (Cornaz et al., 2020a). Not only superior fixation stability was observed with the 3D printed clamps for the fixation of thoracic and lumbar vertebrae (vertebra clamp) compared to potting, but also additional advantages such as exact specimen orientation, simple access to anatomical structures of interest, prevention of specimen heating during the fixation process and the possibility for non-destructive removal of the clamps were noted (Cornaz et al., 2020a). However, the stability of 3D printed vertebra clamps during high volume routine testing remains unknown and further application of this concept for the fixation of sacral bone for biomechanical testing of the lumbosacral transition has not yet been described.

The aim of this study was to verify the effectiveness of the 3D printed vertebra clamps during routine application and to test the stability of the novel 3D printed sacrum clamp. Novelties of this study are the information on fixation rigidity in large volume routine biomechanical testing, the description and evaluation of the novel sacrum clamp and public access to the template files of the different clamp designs (supplementary data).

2. Material and methods

2.1. 3D printed clamps

The method of fixation of lumbar and thoracolumbar cadaveric spinal segments with 3D printed vertebra clamps has been reported in detail elsewhere (Cornaz et al., 2020a) and the same method was

* Corresponding author at: Balgrist University Hospital, Department of Orthopaedics, University of Zurich, Institute for Biomechanics, ETH Zurich, Balgrist Campus, Lengghalde 5, CH - 8008 Zurich, Switzerland.
E-mail address: jonas.widmer@hest.ethz.ch (J. Widmer).

https://doi.org/10.1016/j.jbiomech.2021.110577
Accepted 11 May 2021
Available online 16 June 2021

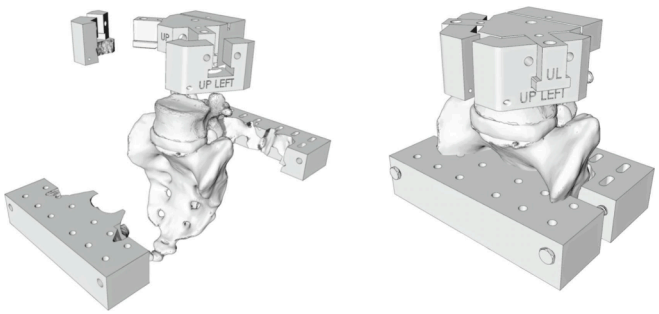

Fig. 1. Visualization of an L5/S1 specimen with a vertebra clamp composed of the base and the two sidepieces for fixation of L5 and a sacrum clamp composed of an anterior and a posterior part for fixation of the sacral bone.

Table 1
Sample size and demographic information on the specimens (age, gender and BMI). For age and BMI the median (min, max) values are reported. (sc = sacrum clamp).

	Sample size	Age [years]	gender	BMI [kg/m^2]
T12/L1	14	68 (45, 90)	5 female, 9 male	27.7 (14.2, 39.2)
L1/2	24	65 (50, 86)	6 female, 18 male	28.9 (16.1, 50)
L2/3	12	68 (45, 82)	3 female, 9 male	27.7 (21, 39.2)
L3/4	24	65 (50, 86)	6 female, 18 male	27.6 (16.1, 50)
L4/5	12	66 (45, 83)	3 female, 9 male	27.7 (21, 33.8)
L5/S1	4	55 (52, 66)	1 female, 3 male	26.5 (24.5, 37.3)
L5/S1$_{sc}$	8	60 (50, 86)	3 female, 5 male	30.3 (16.1, 34.5)
All levels	98	66 (45, 90)	27 female, 71 male	28.1 (14.2, 50)

applied. The same concept was used to design sacral clamps in SolidWorks 2017 (Dassault Systèmes SolidWorks Corp., USA). The clamp was composed of a ventral and dorsal part, which were sized and shaped to roughly follow the concave form of the sacrum and to fully enclose it in the sagittal and frontal plane. Due to the large cranio-caudal extent of the sacrum, it was decided not to enclose the complete bone in this dimension, but to limit the cranio-caudal extent of the clamp to 30 mm and to cut the more caudal aspects of the sacrum. The two parts of the clamp were equipped with hole patterns for clamp compression and for fixation of the clamp in the spine testing setup (Fig. 1).

For specific adaptation of the template, the acquired CT data of the specimens were segmented using 3D Slicer (3D Slicer 4.8.1., www.slicer.org). The generated models of the sacrum and the adjacent vertebral body were then positioned in the template using Blender (Blender Foundation, www.blender.org). After extrusion of the model in the anterior and posterior direction ("Dental3DPlugin Undercut Remove", http://www.amdentalsoft.net), the newly generated models were boolean subtracted from the template to prevent undercutting. The generated clamps were 3D printed with an Original Prusa i3 MK3 printer (Prusa Research s.r.o., Czech Republic) using PLA (polyactic acid) filament with 60% rectangular infill and four vertical shell perimeters.

For firm fixation of the specimens in the 3D printed sacrum clamps, all soft tissue not necessary for later biomechanical testing was removed. After temporal positioning of the clamp for reference, the caudal part of the sacrum was removed with an oscillating saw. The two parts of the clamp were added and compressed with two threaded bars (Fig. 1). The specimens were then mounted into the test rig.

The template files and a more detailed description of the novel 3D printed sacrum clamp as well as the 3D printed vertebra clamp (Cornaz et al., 2020a) are provided as electronic supplementary material.

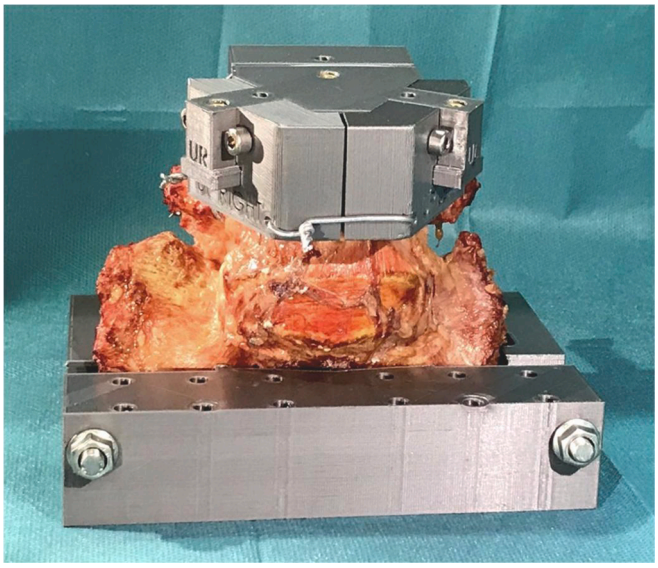

Fig. 2. Picture of an L5/S1 sample fixed with a 3D printed vertebra clamp for the lumbar vertebra and a sacrum clamp for the sacrum.

2.2. Specimen preparation and clamping

The presented data was recorded during routine biomechanical experiments ((Cornaz et al., 2020b; Widmer et al., 2020), unpublished data) performed on a total of 98 single-level spinal segments originating from 40 fresh-frozen human cadavers (Science Care, Phoenix, AZ, USA). The experiments were approved by the local ethical authorities (BASEC Nr. 2017-02018). The specimens were stored at −20° prior to testing. After thawing and sectioning, the thoracic and lumbar vertebrae were clamped according to the previously described method (Cornaz et al., 2020a). The specimens included 14 segments of the thoracolumbar junction (Th12/L1), 72 lumbar segments (24 L1/L2, 12 L2/3, 24 L3/4, 12 L4/5) and 12 segments of the lumbosacral junction (L5/S1) (Table 1). For the fixation of S1 specimens, vertebra clamps were used in 4 cases and sacrum clamps were used in 8 cases. This resulted in a total of 90 segments with two vertebra clamps and 8 segments with a vertebra clamp cranially and a sacrum clamp caudally (Fig. 2).

2.3. Biomechanical testing

Testing was performed at room temperature on a biaxial linear-torsion static testing system (Zwick/Roell Allroundline 10kN, testXpert III software, ZwickRoell GmbH & Co. KG, Germany), which was supplemented with a spine testing setup to generate semi-constrained loading conditions in flexion–extension (FE), lateral bending (LB), axial rotation (AR), anteroposterior shear (AS), lateral shear (LS), axial compression and decompression (AC) (Widmer et al., 2020). Loading was applied with 1 °/sec in FE and LB; 0.5 °/s in AR, 0.5 mm/sec in AS, PS, and LS and 0.1 mm/sec in AC. The loading amplitudes were +/-7.5 Nm in FE, LB and AR, +/-150 N in AS, PS, and LS and + 400/-150 N in AC. During testing (<8h testing time per segment), the specimens were frequently sprayed with PBS to prevent dehydration.

For the evaluation of fixation stability, a 3D motion capture system (Atracsys Fusion Track 500, Artracsys, Switzerland) with a temporal resolution of 10 Hz and a tracking accuracy of 0.09 mm RMS was used to track marker tools equipped with reflective spheres (OptiTrack Motion Capture Markers, MKR064M3-10, NaturalPoint Inc, USA) attached to the two vertebrae and the two clamps. During the last load-controlled testing cycle of the native specimens, the projected movement in the angular planes for FE, LB and AR and in the translational directions for AS, LS and AC were computed, analogue to the method described by Cornaz et al. (Cornaz et al., 2020a). The relative motion between

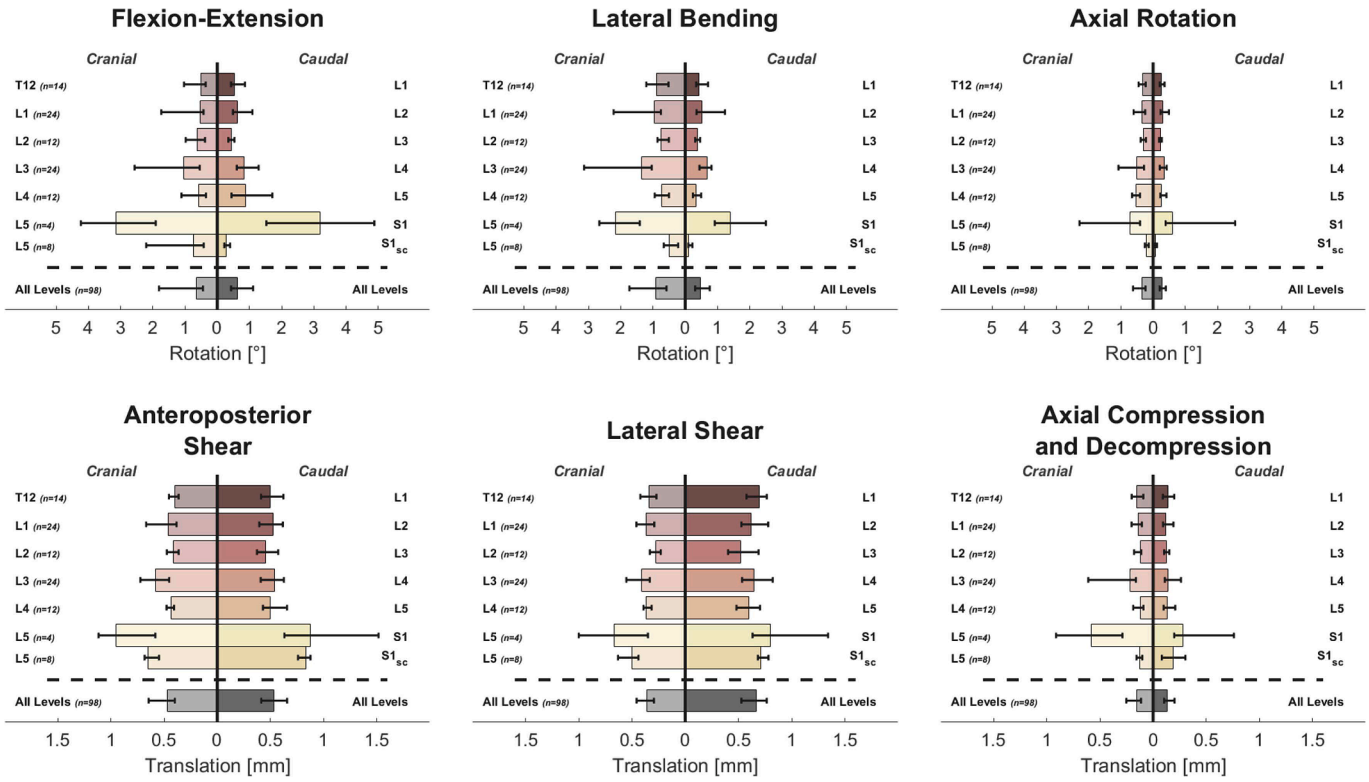

Fig. 3. Bar diagrams of the relative motion between specimen and clamp per anatomical level and as a pooled value for all 98 spinal segments. The specimens fixed which sacrum clamps are marked with the subscript sc (=sacrum clamp). Vertebra clamps were used in all other instances. The height of the bars represents the median, the whiskers represent the 25 and 75 percentiles.

specimen and fixture was computed for each individual clamp as well as for the complete specimen (summed value of the cranial and the caudal clamp).

2.4. Statistical evaluation

The relative motion of the 3D printed clamps in the validation study in which the stability of 3D printed clamps was compared to potting (Cornaz et al., 2020a) was used as benchmark. Statistical evaluation was conducted with Matlab (Matlab R2016b, The MathWorks, Inc., Natick, MA, USA). Since normal distribution could not be assumed for all data according to Shapiro-Wilk tests, two-sided Wilcoxon rank sum tests were used to compare the groups in all 6 loading directions. Statistical significance was assumed with $p < 0.05$.

The summed relative motion of the spinal segments, for which only 3D printed vertebra clamps were used ($n = 90$), was compared to the summed motion of the 3D printed vertebra clamps of the benchmark data ($n = 16$). The fixation stability of all cranial ($n = 98$) and all caudal ($n = 90$) vertebra clamps during routine application were compared to detect differences in fixation stability due to anatomical characteristics. To evaluate the novel 3D printed sacrum clamp, the relative motion of the sacrum clamps ($n = 8$) was compared to the relative motion of the caudal vertebra clamps during routine application ($n = 90$).

3. Results

No mechanical failures of the 3D printed clamps and no movement between the clamps and the test rig was observed during all experiments. The median motion between the vertebra clamps and the specimens was 0.6° in FE, 0.7° in LB, 0.3° in AR, 0.5 mm in AS, 0.5 mm in LS and 0.1 mm in AC. For the sacrum clamps the median motion was 0.3° in FE, 0.1° in LB, 0.08° in AR, 0.8 mm in AS, 0.7 mm in LS and 0.2 mm in AC. The recorded values in dependence of the segmental levels are illustrated in Fig. 3.

Table 2
3D printed vertebra clamp - The median (minimum, maximum) of the summed relative motion for the vertebra clamp during routine application (new data) compared to the benchmark data (Cornaz et al., 2020a). n = sample size.

	New data (n = 90)	Cornaz et al., 2020a, 2020b (n = 16)	Statistics
Flexion-Extension (+/−7.5Nm)	1.5° (0.4°, 14.2°)	2.7° (0.8°, 6.2°)	$p = 0.008$
Lateral Bending (+/−7.5Nm)	1.5° (0.6°, 11.2°)	2.2° (1.1°, 8.0°)	$p = 0.014$
Axial Rotation (+/−7.5Nm)	0.7° (0.3°, 5.2°)	1.0° (0.4°, 1.8°)	$p = 0.028$
Anteroposterior Shear (+/−150 N)	1.0 mm (0.6 mm, 3.2 mm)	1.6 mm (1.3 mm, 2.7 mm)	$p < 0.001$
Lateral Shear (+/−150 N)	1.0 mm (0.6 mm, 2.9 mm)	1.4 mm (1.1 mm, 1.8 mm)	$p < 0.001$
Axial Compression and Decompression (+1500 N/−150 N)	0.3 mm (0.1 mm, 3.0 mm)	0.8 mm (0.5 mm, 1.5 mm)	$p < 0.001$

The summed relative motion of the 90 spinal segments with vertebra clamps during routine application was significantly smaller compared to the benchmark data in all six loading directions (Table 2). Comparing the cranial ($n = 98$) with the caudal ($n = 90$) vertebra clamps, smaller relative motion was observed with the cranial clamps in LS ($p < 0.001$), while the opposite relation was observed in AR and LB ($p < 0.001$). In FE, AS and AC, no significant difference between the stability of the cranial and caudal vertebra clamp was observed ($p > 0.05$).

The relative motion between fixture and specimen with the novel 3D printed sacrum clamp in FE, LB, AR was significantly smaller compared

Table 3
3D printed sacrum clamp - The median (minimum, maximum) of the relative movement between fixture and specimen for the novel sacrum clamp and the caudal vertebra clamp. n = sample size.

	Sacrum Clamp (n = 8)	Caudal vertebra clamp (n = 90)	Statistics
Flexion-Extension (+/−7.5Nm)	0.3° (0.2°, 1.5°)	0.6° (0.1°, 5.8°)	p = 0.002
Lateral Bending (+/−7.5Nm)	0.1° (0.1°, 0.4°)	0.5° (0.1°, 10.7°)	p < 0.001
Axial Rotation (+/−7.5Nm)	0.1° (0.05°, 0.2°)	0.3° (0.1°, 4.4°)	p < 0.001
Anteroposterior Shear (+/−150 N)	0.8 mm (0.7 mm, 0.9 mm)	0.5 mm (0.3 mm, 2.3 mm)	p < 0.001
Lateral Shear (+/−150 N)	0.7 mm (0.7 mm, 0.9 mm)	0.6 mm (0.3 mm, 1.8 mm)	p = 0.080
Axial Compression and Decompression (+1500 N/−150 N)	0.2 mm (0.07 mm, 0.4 mm)	0.1 mm (0.05 mm, 1.2 mm)	p = 0.730

to the caudal 3D printed vertebra clamp, while in AS, the relative motion was larger. In LS and AC statistical significance was not reached (Table 3).

4. Discussion

Accurate and reliable specimen fixation is a relevant factor for biomechanical experiments. 3D printed clamps were proposed as an alternative to potting as they provide the ability to accurately plan specimen orientation, can be adapted to provide simple access to anatomical structures, do not cause specimen heating or require screw insertion and provide the possibility of non-destructive removal (Cornaz et al., 2020a). Superior mechanical performance of 3D printed vertebra clamps compared to potting was demonstrated previously in a pilot study (Cornaz et al., 2020a). The data on relative motion at the specimen-clamp interface served as benchmark for this study to test the performance of routine application of the 3D printed vertebra clamps. Further, a novel 3D printed sacrum clamp was developed and tested and public access to the template files is given.

The relative motion recorded with the 3D printed vertebra clamps during routine application was significantly smaller in all six loading directions compared to the benchmark data (Cornaz et al., 2020a). This demonstrates the effectiveness of 3D printed vertebra clamps during routine application and further implies increased reliability with gained experience. The fixation stability of the cranial clamps was superior in lateral shear loading compared to the caudal clamps, while the fixation stability of the caudal clamps was superior in axial rotation and lateral bending. We assume these differences to be the result of anatomical differences, which could be addressed by specific changes to the design of the cranial and caudal clamps to further increase stability. No mechanical failure of the 3D printed vertebra clamps and no loosening of the specimens occurred during testing, which was a relevant problem with potting (Cornaz et al., 2020a). However, the summed relative motion of some specimens was comparably large with maximum values reaching 14.2° in FE and 11.2° in LB (Table 2). These outliers show that despite good general fixation stability, specimen fixation is not perfect in all cases. Additional options in the template files of the 3D printed vertebra clamps could be developed to help optimize the fixation strength in situation with anatomical peculiarities (e.g. spondylophytes), strongly tilted specimens (e.g. degenerative scoliosis) or in situations with larger lumbar lordosis angles (e.g. in L5/S1).

No direct comparison was performed to compare 3D printed clamps to alternative fixation methods such as potting, screw augmented potting or simple screw fixation for the sacrum. However, the stability of the novel 3D printed sacrum clamp was superior compared to the caudal vertebra clamp during routine application in flexion–extension, lateral bending and axial rotation. This could partially be explained by the larger cranio-caudal contact area with sacrum clamps (30 mm) compared to vertebra clamps (~25 mm). In anteroposterior shear loading, the stability of the sacrum clamps was inferior compared to the caudal vertebra clamps, while the maximal motion was still below 1 mm in this loading direction, compared to the maximum value of 2.3 mm with the vertebra clamps (Table 3). Overall, it can be conclude that novel 3D printed sacrum clamps provide a reliable fixation of the sacral bone during biomechanical experiments. While the applied loading amplitudes were chosen to represent physiological loading conditions, higher or different loads can occur in-vivo. The efficacy of the 3D printed clamps could differ with such loading conditions.

In conclusion, 3D printed clamps represent a reliable method for the routine fixation of thoracolumbar and lumbar vertebrae as well as for the fixation of the sacrum during biomechanical testing. Since motion between specimens and clamps cannot be eliminated completely, the concomitant use of a 3D motion capture system appears essential. The template files of the 3D printed clamps are provided as electronic supplementary material.

Declaration of Competing Interest

The authors declare that they have no known competing financial interests or personal relationships that could have appeared to influence the work reported in this paper.

Acknowledgements

The authors gratefully acknowledge the contribution of Mauro Suter for his support during biomechanical testing. This study was not funded by third parties.

Appendix A. Supplementary data

Supplementary data to this article can be found online at https://doi.org/10.1016/j.jbiomech.2021.110577.

References

Cornaz, F., Fasser, M.R., Spirig, J.M., Snedeker, J.G., Farshad, M., Widmer, J., 2020a. 3D printed clamps improve spine specimen fixation in biomechanical testing. J. Biomech. 98, 109467 https://doi.org/10.1016/j.jbiomech.2019.109467.

Cornaz, F., Widmer, J., Farshad-Amacker, N.A., Spirig, J.M., Snedeker, J.G., Farshad, M., 2020b. Biomechanical Contributions of Spinal Structures with Different Degrees of Disc Degeneration. Spine (Phila. Pa. 1976) 1. https://doi.org/10.1097/BRS.0000000000003883.

Widmer, J., Cornaz, F., Scheibler, G., Spirig, J.M., Snedeker, J.G., Farshad, M., 2020. Biomechanical contribution of spinal structures to stability of the lumbar spine—novel biomechanical insights. Spine J. 20, 1705–1716. https://doi.org/10.1016/j.spinee.2020.05.541.